Cylindrical Substrate Microstrip Line Characterization

NICÓLAOS G. ALEXÓPOULOS, FELLOW, IEEE, AND AKIFUMI NAKATANI, STUDENT MEMBER, IEEE

Abstract—**In this article, quasi-static and dynamic solutions are derived for microstrip transmission lines on circularly symmetric cylindrical substrates. Novel numerical techniques have evolved which lead to very efficient algorithms. The model is applicable to substrates of arbitrary thickness and cylinder size. Furthermore, it has been checked against a variety of limiting cases, including microstrip on a flat substrate, and it has been found to provide results with excellent accuracy. The analytical extraction of the quasi-static behavior from the dynamic Green's function introduces considerable simplicity in developing the algorithm.**

I. INTRODUCTION

THE DESIGN OF microstrip antennas and microstrip antenna arrays on cylindrically shaped substrates necessitates the development of highly accurate design procedures not only for the microstrip antennas, but also for the microstrip circuitry which forms the antenna or array excitation network. This article presents the development of a dynamic model for a microstrip transmission line printed on a circularly symmetric cylindrical substrate. A quasi-static model has also been derived so as to provide an investigation of the computational accuracy of the dynamic Green's function. It is determined that the algorithm provides excellent accuracy and that it agrees with all limiting cases, including the configuration of microstrip on flat substrates. Quasi-static models for microstrip on cylindrical substrates have been obtained previously with good accuracy by conformal mapping [1], [2] and by numerical solution to Laplace's equation [3]. These models however are useful for the computation of the static parameters of the microstrip line, such as capacitance, and they should not be used for the evaluation of the frequency-dependent properties of such a complicated waveguiding structure on a cylindrical substrate. The quasi-static and dynamic solutions developed in this article rely on the development of the Green's function and the solution of the pertinent integral equation by numerical techniques such as the method of moments [4]–[7].

The most significant issue in the attempt to characterize the microstrip transmission line on a cylindrical substrate is the development of an accurate numerical procedure for the computation of the pertinent Green's function. Specifically, a breakthrough has been needed for some time now, which will lead to the calculation of the near fields generated by a printed current line source (two-dimensional problem) or by a printed electric dipole (three-dimensional problem) with the desired accuracy. This was achieved recently for microstrip dipole antennas printed on a cylindrical substrate [8], [9]. There, a highly efficient algorithm was developed which provides convergent numerical evaluation of the pertinent Green's function with the desired accuracy. This algorithm has been modified to address the two-dimensional (2-D) waveguiding problem of the infinite microstrip line on a cylindrical substrate, i.e., the principal problem of concern in this article. To this end, the Green's function is derived for the quasi-static as well as for the dynamic model, and the similarity of the functional behavior of both Green's functions is discussed in detail. The algorithm is based on extracting the dominant behavior of the Green's function and on the judicious use of recurrence relations and continued fraction representations of the Bessel-type functions involved in the problem. This algorithm is general so that it provides highly accurate solutions for all conceivable limiting cases, such as the static problem, arbitrarily thin or thick substrate, and arbitrary cylinder size. Furthermore, it has been checked against the planar microstrip configuration, two-wire line, a wire above a planar conductor, and the parallel-plate line, providing excellent agreement with each limiting case.

Manuscript received January 13, 1987; revised April 13, 1987. This work was supported by the National Science Foundation under Grant ECS 86 04837.

The authors are with the Electrical Engineering Department, University of California at Los Angeles, Los Angeles, CA 90024.

IEEE Log Number 8715976.

II. THE QUASI-STATIC PROBLEM FORMULATION

The geometry of interest is shown in Fig. 1, which depicts a cylindrical substrate with inner and outer radii ρ_1 and ρ_2, respectively, and relative dielectric constant ϵ_r. The width of the infinitely long microstrip line is denoted as $w = \rho_2\delta_\phi$, where δ_ϕ is the angular extent of the strip defined in the figure. The Green's function to the static problem is obtained by considering as the source of potential an infinite line of unit charge at $\rho = \rho_2$ and $\phi = \phi'$. The Poisson equation

$$\left\{\frac{1}{\rho}\frac{\partial}{\partial\rho}\left(\rho\frac{\partial}{\partial\rho}\right)+\frac{1}{\rho^2}\frac{\partial^2}{\partial\phi^2}\right\}g(\rho,\phi) = -\frac{\delta(\rho-\rho_2)}{\epsilon_r\epsilon_0\rho}\delta(\phi-\phi') \quad (1)$$

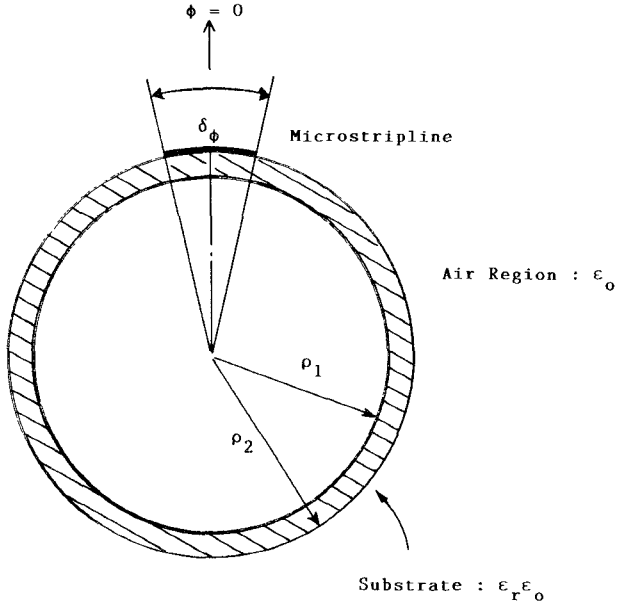

Fig. 1. Cylindrical substrate microstrip configuration. $R = \rho_1/\rho_2$.

is solved by substituting the Fourier series representation

$$g(\rho,\phi) = \sum_{m=-\infty}^{+\infty} \tilde{g}(\rho,m)\exp(jm\phi) \tag{2}$$

in (1). The boundary conditions are written in the spectral domain as

$$\tilde{g}^{(1)}(\rho_2,m) = \tilde{g}^{(0)}(\rho_2,m) \tag{3}$$

and

$$\frac{d}{d\rho}\left\{\tilde{g}^{(0)}(\rho,m) - \epsilon_r\tilde{g}^{(1)}(\rho,m)\right\}_{\rho=\rho_2} = -\frac{\exp(-jm\phi')}{2\pi\rho_2}. \tag{4}$$

The Green's function is readily obtained as

$$g(\rho_2,\phi) = \frac{1}{2\pi\epsilon_0}\left\{\frac{1}{\epsilon_r}\log(1/R) + 2\sum_{m=1}^{+\infty}\frac{\cos[m(\phi-\phi')]}{m[1+\epsilon_r\coth(m\log(1/R))]}\right\} \tag{5}$$

where $R = \rho_1/\rho_2$. The microstrip potential is related to the charge density distribution per unit length $\rho_l(\phi)$ through the integral equation

$$V_0 = V(\phi) = \int_{-\delta_\phi/2}^{\delta_\phi/2} g(\phi-\phi')\rho_l(\phi')\,d\phi'. \tag{6}$$

The Galerkin method is applied to solve the integral equation for the unknown charge density by expressing $\rho_l(\phi')$ as a series of pulse basis functions with unknown coefficients a_j. The integral equation is therefore reduced to a system of algebraic equations in the form

$$[V_i] = [Z_{i,j}][a_j], \qquad i,j = 1,2,\cdots,N \tag{7}$$

where $V_i = V_0 = 1$, and the matrix elements $Z_{i,j}$ are given by

TABLE I
CLAUSEN'S COEFFICIENTS OF EQUATION (13)

n	c_n	n	c_n
1	0.75	5	1.4822216 (-9)
2	3.4722222 (-3)	6	1.5815725 (-11)
3	1.1574074 (-4)	7	2.4195010 (-13)
4	9.8418997 (-8)	8	3.9828978 (-15)

$$Z_{i,j} = \frac{\log(1/R)}{2\pi\epsilon_0\epsilon_r} + \frac{4\Lambda_{i,j}}{\pi\Delta\epsilon_0(\epsilon_r+1)} + \frac{4}{\pi\Delta\epsilon_0}\sum_{m=1}^{+\infty}\frac{1}{m^3} \cdot\left\{\frac{1}{1+\epsilon_r\coth(m\log(1/R))} - \frac{1}{(1+\epsilon_r)}\right\} \cdot\sin^2\left(\frac{m\Delta}{2}\right)\cos\left[m(\phi_i-\phi_j)\right]. \tag{8}$$

In (8) the parameter Δ denotes the pulse expansion function width, while $\Lambda_{i,j}$ is the sum

$$\Lambda_{i,j} = \sum_{m=1}^{+\infty}\frac{1}{m^3}\sin^2\left(\frac{m\Delta}{2}\right)\cos\left[m(\phi_i-\phi_j)\right]. \tag{9}$$

The quantity $\Lambda_{i,j}$ may be cast into the following representation to facilitate computation:

$$\Lambda_{i,j} = \frac{1}{2}\left[Y_1 - \frac{1}{2}(Y_2+Y_3)\right] \tag{10}$$

where Y_i $(i=1,2,3)$ is defined as

$$Y_i = \sum_{m=1}^{+\infty}\frac{\cos(mX_i)}{m^3} \tag{11}$$

with

$$X_1 = \phi_i - \phi_j \quad X_2 = X_1 + \Delta \quad \text{and} \quad X_3 = X_1 - \Delta. \tag{12}$$

The form Y_i may be computed by using Clausen's integral and related summation form [10], [11], i.e.,

$$Y(X) = 1.2020569 + 0.5X^2\log(X) - \sum_{n=1}^{\infty} c_n X^{2n} \tag{13}$$

with c_n obtaining values such as those shown in Table I for the first eight coefficients.

III. DISPERSIVE MODEL

The dispersive model for the microstrip line shown in Fig. 1 is obtained by using the spectral method to solve Maxwell's equations in the cylindrical coordinate system. The electromagnetic field components are expressed in the spectral domain as

$$\tilde{E}_\rho = \frac{jk_z}{\gamma^2}\frac{\partial\tilde{E}_z}{\partial\rho} + \frac{m\omega\mu_0}{\gamma^2\rho}\tilde{H}_z \tag{14}$$

$$\tilde{E}_\phi = -\frac{mk_z}{\gamma^2\rho}\tilde{E}_z + \frac{j\omega\mu_0}{\gamma^2}\frac{\partial\tilde{H}_z}{\partial\rho} \tag{15}$$

$$\tilde{H}_\rho = -\frac{m\omega\epsilon_r\epsilon_0}{\gamma^2\rho}\tilde{E}_z + \frac{jk_z}{\gamma^2}\frac{\partial\tilde{H}_z}{\partial\rho} \tag{16}$$

$$\tilde{H}_\phi = -\frac{j\omega\epsilon_r\epsilon_0}{\gamma^2}\frac{\partial\tilde{E}_z}{\partial\rho} - \frac{mk_z}{\gamma^2\rho}\tilde{H}_z \tag{17}$$

where $\tilde{E}_z$ and $\tilde{H}_z$ satisfy the wave equation

$$\left\{\frac{1}{\rho}\frac{d}{d\rho}\left(\rho\frac{d}{d\rho}\right)+\left(\gamma_{(i)}^2-\frac{m^2}{\rho^2}\right)\right\}\tilde{\Psi}^{(i)}=0. \tag{18}$$

Here $\tilde{\Psi}^{(i)}$ represents $\tilde{E}_z^{(i)}$ or $\tilde{H}_z^{(i)}$ and $\gamma_i^2=k_i^2-k_z^2$, with $i=1,0$ denoting the substrate or free-space region, respectively. The boundary conditions at $\rho=\rho_2$ yield

$$\tilde{E}_z^{(1)}=\tilde{E}_z^{(0)} \tag{19}$$

and

$$\hat{\rho}\times\left(\tilde{\vec{H}}_t^{(1)}-\tilde{\vec{H}}_t^{(0)}\right)=\tilde{\vec{J}}_s \tag{20}$$

where $\tilde{\vec{J}}_s$ is the Fourier transform of $\vec{J}_s=\hat{\phi}J_\phi+\hat{z}J_z$. The unknown current density $\vec{J}$ may be obtained by solving the system

$$\begin{bmatrix}\tilde{E}_\phi^{(0)}\\ \tilde{E}_z^{(0)}\end{bmatrix}=\begin{bmatrix}G_{\phi\phi}^{(0)} & G_{\phi z}^{(0)}\\ G_{z\phi}^{(0)} & G_{zz}^{(0)}\end{bmatrix}\begin{bmatrix}\tilde{J}_\phi\\ \tilde{J}_z\end{bmatrix} \tag{21}$$

for $\tilde{J}_\phi$ and $\tilde{J}_z$ on the strip. The dynamic Green's function components $G_{\phi\phi}^{(0)}$, $G_{\phi z}^{(0)}$, $G_{z\phi}^{(0)}$, and $G_{zz}^{(0)}$ are given in the Appendix, for convenience. Since we assume the strip to be narrow (i.e., $w\ll\lambda_g$), J_ϕ may be neglected [7]. Galerkin's method is used to yield results for the effective dielectric constant $\epsilon_{\text{eff}}=(k_z/k_0)^2$. The line characteristic impedance is calculated by adopting the definition $Z_0=V_0/I_z$, where I_z is the total longitudinal current on the strip and V_0 is the potential difference of the strip to ground. A stationary expression may be derived for Z_0 as follows. The electric field component E_ρ is given by

$$E_\rho^{(1)}(\rho,\phi)=\sum_{-\infty}^{+\infty}\tilde{E}_\rho^{(1)}\exp(jm\phi) \tag{22}$$

where

$$\tilde{E}_\rho^{(1)}=G_{\rho z}^{(1)}(\rho,m)\tilde{J}_z(m). \tag{23}$$

Since the potential on the strip is given by

$$V(\phi)=\int_{\rho_2}^{\rho_1}E_\rho^{(1)}(\rho,\phi)\,d\rho \tag{24}$$

if we define

$$\tilde{V}_m=\int_{\rho_2}^{\rho_1}G_{\rho z}^{(1)}(\rho,m)\,d\rho \tag{25}$$

and

$$V(\phi)=\sum_{-\infty}^{+\infty}\tilde{V}_m\tilde{J}_z(m)\exp(jm\phi) \tag{26}$$

then application of Galerkin's method to (26) will result in

$$V_0=\frac{2\pi\rho_2}{I_z}\sum_{-\infty}^{+\infty}\tilde{V}_m\tilde{J}_z(m)\tilde{J}_z^*(m). \tag{27}$$

Therefore Z_0 is

$$Z_0=\frac{2\pi\rho_2}{I_z^2}\sum_{-\infty}^{+\infty}\tilde{V}_m\tilde{J}_z(m)\tilde{J}_z^*(m) \tag{28}$$

which is the stationary result. The expression for $\tilde{V}_m$ is found as

$$\tilde{V}_m=-\frac{\sqrt{\epsilon_{\text{eff}}}\gamma_0\eta}{\gamma_1^2}\left\{\left(\frac{N_m^{12}}{D_m}\right)-\frac{m^2}{D_m}\frac{k_0^2(\epsilon_r-1)}{\gamma_1^2(\gamma_0\rho_2)}H_m\right\} \tag{29}$$

where H_m is given by

$$H_m=\int_{\rho_2}^{\rho_1}\frac{h_m(\gamma_1\rho)}{\rho h_m(\gamma_1\rho_2)}\,d\rho \tag{30}$$

with parameters defined in the Appendix:

$$h_m(\gamma_1\rho)=N_m'(\gamma_1\rho_1)J_m(\gamma_1\rho)-J_m'(\gamma_1\rho)N_m(\gamma_1\rho) \tag{31}$$

and η represents the free-space wave impedance. It is interesting to note that at the quasi-static limit this expression reduces to

$$Z_0=\frac{\sqrt{\epsilon_{\text{eff}}}\eta}{2\pi\epsilon_r}\cdot\left\{\log(1/R)+2\epsilon_r\sum_{m=1}^{+\infty}\frac{\bar{I}(m)}{m[1+\epsilon_r\coth(m\log(1/R))]}\right\} \tag{32}$$

where

$$\bar{I}(m)=\frac{\langle\exp(jm\phi),J_z(\phi),\exp(-jm\phi')\rangle}{\langle J_z(\phi),1\rangle} \tag{33}$$

with $\langle\ \rangle$ denoting inner product. If pulse basis functions are used as expansion functions with width Δ, then

$$\bar{I}(m)=\operatorname{sinc}\left(\frac{m\Delta}{2}\right)\operatorname{sinc}\left(\frac{m\delta_\phi}{2}\right)\frac{\sum_{n=1}^{N}a_n\cos(m\phi_n)}{\sum_{n=1}^{N}a_n} \tag{34}$$

where $\operatorname{sinc}(x)=\sin(x)/x$, δ_ϕ is the width of the line, and a_n are the unknown coefficients in the current expansion. When the microstrip line is extended so that its width $\delta_\phi=2\pi$, the coaxial line is obtained. For this case, $\epsilon_{\text{eff}}=\epsilon_r$, $\operatorname{sinc}(m\delta_\phi/2)=0$; i.e., $\bar{I}(m)=0$ and the expression for the characteristic impedance reduces to the first term of (32), i.e.,

$$Z_0=\frac{60}{\sqrt{\epsilon_r}}\log\left(\frac{\rho_2}{\rho_1}\right). \tag{35}$$

IV. Algorithm Description

An efficient algorithm can be developed by considering an approach which bypasses the need to compute directly Bessel-type functions for any order and/or argument. This is achieved by computing equations (A11) and (A12) in the Appendix. It is useful to note that these equations yield, when properly combined, the term $\coth[m\log(1/R)]$ in the quasi-static solution. Furthermore, it should be observed that the wave equation reduces to Laplace's equation when the argument of the Bessel-type functions involved is small or the order is large. The development of the algorithm becomes clearer by considering, as an example, the manipulations introduced for the computation of

$Y_m^{(1)}$. The expression for $Y_m^{(1)}$ may be written, by using the Wronskian and recursive relations, as

$$Y_m^{(1)} = Y_{m0}^{(1)} - \Delta Y_m^{(1)} \tag{36}$$

where

$$Y_{m0}^{(1)} = \frac{m}{\gamma_1\rho_2} - \frac{J_{m+1}(\gamma_1\rho_2)}{J_m(\gamma_1\rho_2)} \tag{37}$$

and

$$\Delta Y_m^{(1)} = \frac{2}{\pi\gamma_1\rho_2} \frac{J_m(\gamma_1\rho_1)/J_m(\gamma_1\rho_2)}{N_m(\gamma_1\rho_1)J_m(\gamma_1\rho_2) - N_m(\gamma_1\rho_2)J_m(\gamma_1\rho_1)}. \tag{38}$$

The asymptotic expression of (38) is derived as

$$\Delta Y_m^{(1)} \Rightarrow \frac{2}{\gamma_1\rho_2} \frac{m}{1-R^{-2m}} \tag{39}$$

where the combination of the first term in $Y_{m0}^{(1)}$ and (39) yields the corresponding quasi-static behavior of the function. Now, the dominant and perturbation terms are defined as

$$y_{m0}^{(1)} = \frac{m}{\gamma_1\rho_2}\coth\left[m\log(1/R)\right] - \frac{J_{m+1}(\gamma_1\rho_2)}{J_m(\gamma_1\rho_2)} \tag{40}$$

and

$$\Delta y_m^{(1)} = \frac{2}{\gamma_1\rho_2}\left[\frac{\frac{1}{\pi}J_m(\gamma_1\rho_1)/J_m(\gamma_1\rho_2)}{N_m(\gamma_1\rho_1)J_m(\gamma_1\rho_2) - N_m(\gamma_1\rho_2)J_m(\gamma_1\rho_1)} - \frac{m}{1-R^{-2m}}\right]. \tag{41}$$

The dominant terms are computed by using the continued fraction method, where only the ratio of Bessel's functions is required. The computation of the perturbation term is performed by forming a new recurrence relation in the following manner; when the ratios p_m and q_m are defined as

$$p_m = \frac{J_{m+1}(z)}{J_m(z)} \tag{42a}$$

and

$$q_m = \frac{N_{m+1}(z)}{N_m(z)} \tag{42b}$$

then the recurrence relation is obtained as

$$G_{m+1}^{(1)} = \frac{q_m(A)p_m(B)}{p_m(A)q_m(B)} G_m^{(1)} \tag{43}$$

with

$$G_0^{(1)} = \frac{N_0(A)J_0(B)}{J_0(A)N_0(B)} \tag{44}$$

and

$$\Delta y_m^{(1)} = \left\{\frac{p_m(B) - q_m(B)}{G_m^{(1)} - 1} - \frac{2}{B}\frac{m}{1-R^{-2m}}\right\}. \tag{45}$$

Now the term $Y_m^{(1)}$ is computed by using (40) and (45) as

$$Y_m^{(1)} = y_{m0}^{(1)} - \Delta y_m^{(1)} \tag{46}$$

where $A = \gamma_1\rho_1$ and $B = \gamma_1\rho_2$. Here forward recurrence applies to $q_m(z)$ and $G_m^{(1)}$ while the continued fraction relation applies to the Bessel function of the first kind. The benefits of using these relations are: (a) one can determine the accuracy for arbitrary order and argument (including complex argument) explicitly, (b) subroutines for computing these functions can be coded very efficiently, and (c) one needs to compute only zero-order Bessel functions to calculate $G_0^{(1)}$ or a simple program may be written separately to achieve the same goal. The term defined in (45) yields faster convergence; i.e., the quantities are much smaller than the dominant term defined in (40).

V. Numerical Results

A variety of limiting cases is presented in this section to demonstrate the accuracy and versatility of the developed analysis and algorithm. The Galerkin procedure is applied for the quasi-static as well as dynamic solutions, with pulse basis functions being chosen as both expansion and testing functions. The number of basis functions is chosen as 40 for half of the strip width and this leads to better than 0.5 percent convergence accuracy for both the quasi-static and dynamic solutions.

A. Quasi-Static Simulation

The first three examples demonstrate how the cylindrical solutions approach in the limit the two-wire transmission line, the wire above a ground plane, and the parallel-plate transmission line solutions. The characteristic impedance for the quasi-static solution is obtained by using (7) or by using the current distribution when ϵ_r approaches unity in the dynamic solution.

1) Two-Wire Transmission Line: If $\epsilon_r = 1$, $R \ll 1$, $w/H \ll 1$, and $\rho_2 \gg \rho_1$, the geometry approaches that of the two-wire transmission line. The characteristic impedance of such a line is given by $Z_0 = 120\cosh^{-1}(D/d)$, where D is the distance between the wires and d is the diameter of the wire. At the limit $Z_0 \to 120\ln(1/R)$ when $R \ll 1$ and $w/H \ll 1$ with $w = 4\rho_1$. Table II shows the manner in which the microstrip above a cylinder approaches the two-wire transmission line.

2) Strip Above a Planar Geometry: If $\epsilon_r = 1$, $w/H \ll 1$, and R approaches unity, then the solution tends to that of the strip above a ground plane. The characteristic impedance for this geometry is given by the expression

$$Z_0 = 60\log\left\{\frac{8(\rho_2 - \rho_1)}{w}\right\}. \tag{47}$$

When $w/H = 10^{-4}$, this formula yields $Z_0 = 677.4\ \Omega$. The algorithm approaches the theoretical value, as shown in

TABLE II
TWO-WIRE SIMULATION

R	Z_0 (Two wire)	Z_0 (This algorithm)
0.1	276.3	282.1
0.01	552.6	553.0
0.001	828.9	828.6
0.0001	1105.2	1105.2

TABLE III
WIRE ABOVE A GROUND PLANE

R	Z_0 (Ohms)	% Diff.
0.7	689.2	1.74
0.9	680.8	0.50
0.99	677.8	0.06
0.995	677.4	0.00

TABLE IV
PARALLEL-PLATE SIMULATION

W/H	Z_0 (Formula)	Z_0 (Model)
50	7.540	7.053
100	3.770	3.637
200	1.885	1.850
400	0.942	0.934
600	0.628	0.625

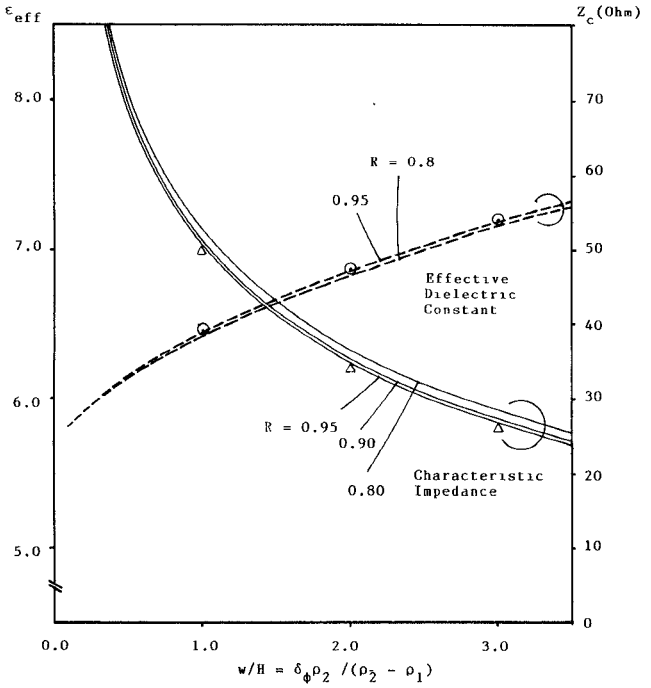

Fig. 2. Low-frequency properties ($\epsilon_r = 9.6$). Planar geometry. $R = 1.0$ [6].

Table III. The results obtained here reveal how the curved surface affects the circuit parameters. When the circuit dimension is small compared to the cylinder diameter, it essentially simulates the planar geometry. This means that the local field, defined as the field in the vicinity of the circuit, dominates the transmission line properties independent of frequency.

3) Parallel-Plate Line: When $w/H \gg 1$, the geometry approaches a parallel-plate line. For this type of line $Z_0 = 120\ \pi\ (H/w)$. A comparison of the two cases is shown in Table IV for $R = 0.995$. As the table indicates, the characteristic impedance computation by the algorithm for a metallic strip above a cylindrical conductor converges to the result of the parallel-plate line as $w/H \gg 1$ and $R \to 1$. Although additional limiting cases may be considered, it is instructional at this point to present a few new results in graphical form. Fig. 2 shows the quasi-static behavior of ϵ_{eff} and Z_0 versus w/H for $\epsilon_r = 9.6$ and $R = 0.8$, 0.9, and 0.95, respectively. Superimposed on this figure are data for the corresponding cases of microstrip on a planar substrate [6]. The figure indicates clearly that as $R \to 1$ the planar geometry is simulated with very high accuracy.

TABLE V
LOW-FREQUENCY SIMULATION

	Quasi-static		Dynamic		[2]	
w/H	Zo	ϵ_{eff}	Zo	ϵ_{eff}	Zo	ϵ_{eff}
1.0	51.15	6.425	51.22	6.426	51.21	6.566
1.5	41.49	6.660	41.60	6.663	40.43	6 818
2.0	35.10	6.860	35.33	6.868	34.45	7.018

TABLE VI
CURVILINEAR EFFECT AT LOW FREQUENCY

R	Z_0	% Diff.	ϵ_{eff}	% Diff.	k_0
0.5	58.96	18.37	6.482	0.65	0.01
0.6	56.44	13.32	6.436	0.06	0.01
0.9	51.15	2.69	6.425	0.23	0.01
0.94	50.61	1.61	6.433	0.11	0.1
0.98	50.10	0.59	6.442	0.03	0.1
0.99	49.98	0.35	6.444	0.06	0.1

B. Frequency-Dependent Simulation

The dynamic solution is compared with the quasi-static case discussed in this article as well as with the results presented in [8]. The substrate is assumed to have a relative dielectric constant $\epsilon_r = 9.6$, $R = 0.9$, and $k_0 = 0.01$. The condition $k_0 \ll 1$ simulates the low-frequency limit. Table V presents the comparison for $w/H = 1.0$, 1.5, and 2.0, respectively, where $w = \delta_\phi \rho_2$ and $H = \rho_2 - \rho_1$. The table indicates very good agreement between the dynamic and quasi-static solutions presented here, while the results in [2] are better than 2 percent higher in the evaluation of ϵ_{eff}.

The manner in which the present algorithm approaches these values is shown in Table VI for $w/H = 1.0$. The equivalent planar geometry in the quasi-static case yields $\epsilon_{eff} = 6.4403$ and $Z_0 = 49.981$ [6], where the circuit dimensions are matched for both geometries. This table demonstrates that Z_0 is very sensitive to the value of R. Fig. 3 shows the dispersive behavior of ϵ_{eff} and Z_0 versus $k_0 b$ for $\epsilon_r = 9.6$, $R = 0.9$, and $w/H = 1.0$, 1.5, and 2.0, respectively. A few planar configuration points are also shown for comparison (the circuit parameters of the planar geometry are matched to the corresponding ones of microstrip on a cylindrical substrate). Fig. 4 is similar to Fig. 3 but for a RT-Duroid substrate with $\epsilon_{eff} = 2.32$. Strong dispersive behavior is observed for the higher dielectric constant. Another interesting result is presented in Fig. 5, where the capacitance per unit length of the microstrip line normalized to the capacitance of the coaxial line is shown

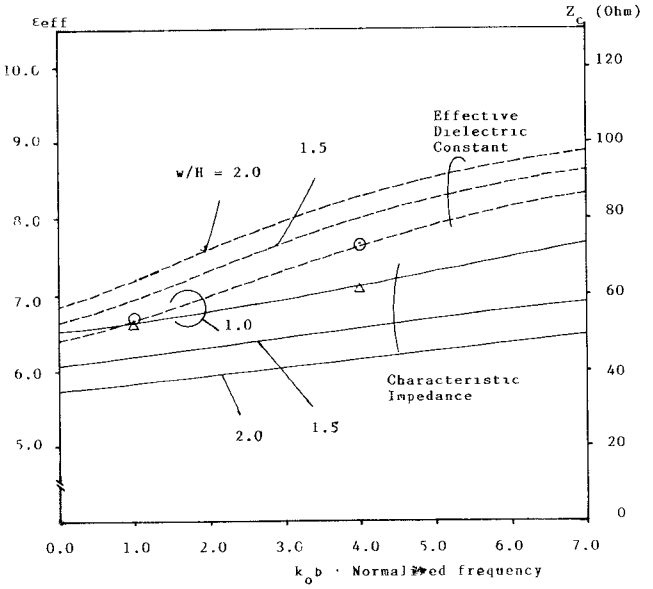

Fig. 3. Frequency-dependent properties (alumina). $\epsilon_r = 9.6$ and $R = 0.9$ Planar geometry. $R = 1.0$ [6].

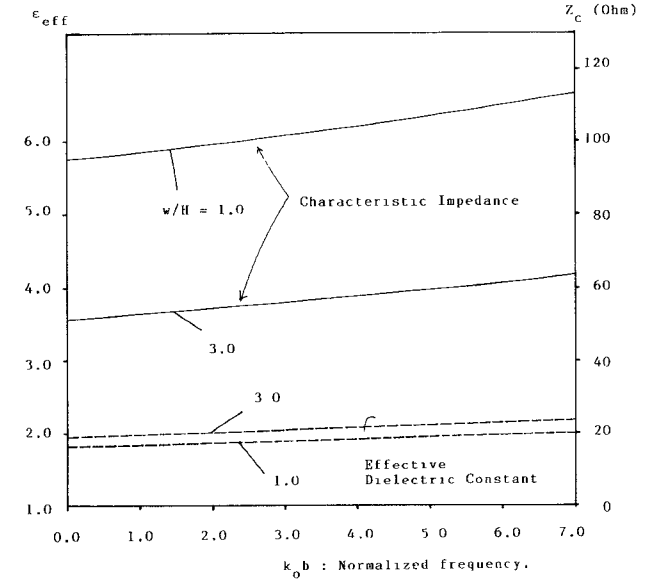

Fig. 4 Frequency-dependent properties. $\epsilon_r = 2.32$ (RT/Duroid) and $R = 0.9$.

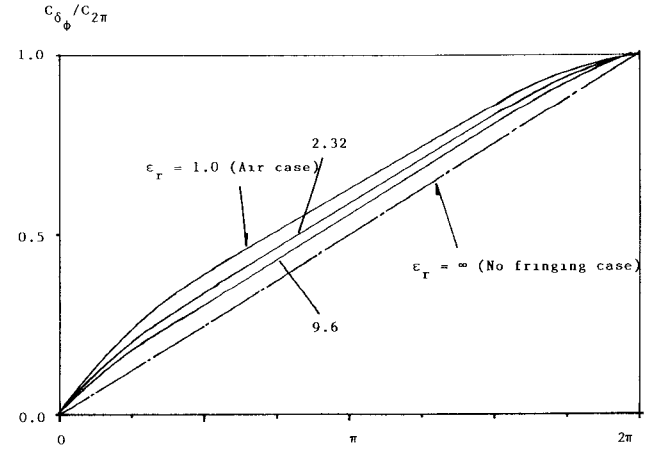

Fig. 5. Normalized capacitance of the line. $R = 0.7$.

versus δ_ϕ. $C_{\delta\phi}$ approaches, as expected, the linear variation (no fringing) as $\epsilon_r \gg 1$. These curves (Fig. 5) may be used to determine the effective width of the line.

VI. Conclusions

A highly accurate method has been developed for the computation of the dynamic Green's functions on a circularly symmetric cylindrical substrate. The method is applied for the computation of the dispersive properties of single microstrip line on a dielectric substrate. The solution is obtained by applying the Galerkin method to the resulting integral equation for both the quasi-static and the dispersive case. A closed-form solution is obtainable in the same fashion for both cases. The efficiency of the solution relies on the accurate computation of the Green's function on the substrate surface for both source and observation points. For the cylindrical substrate geometry, this is achieved by using the continued fraction representation of the Bessel function of the first kind and recurrence representation of the Bessel function of the second kind; these are modified to compute the functions directly without evaluating individual Bessel functions. The algorithm has been verified for a variety of limiting cases with excellent agreement. Finally, a useful stationary expression has been derived for the characteristic impedance analytically, and it has been shown that it yields at the limit the expression of the characteristic impedance for the coaxial line.

Appendix

The dyadic Green's function components in (21) are obtained as

$$G_{\phi\phi}^{(0)} = \frac{jk_0\eta}{\gamma_0}\left[\left(\frac{N_m^{21}}{D_m}\right)\frac{H_m^{(2)\prime}(\gamma_0\rho)}{H_m^{(2)}(\gamma_0\rho_2)} - \frac{mk_z}{k_0^2\rho}\left(\frac{N_m^{22}}{D_m}\right)\frac{H_m^{(2)}(\gamma_0\rho)}{H_m^{(2)}(\gamma_0\rho_2)}\right] \tag{A1}$$

$$G_{\phi z}^{(0)} = \frac{jk_0\eta}{\gamma_0}\left[\left(\frac{N_m^{11}}{D_m}\right)\frac{H_m^{(2)\prime}(\gamma_0\rho)}{H_m^{(2)}(\gamma_0\rho_2)} - \frac{mk_z}{k_0^2\rho}\left(\frac{N_m^{12}}{D_m}\right)\frac{H_m^{(2)}(\gamma_0\rho)}{H_m^{(2)}(\gamma_0\rho_2)}\right] \tag{A2}$$

$$G_{z\phi}^{(0)} = \frac{j\gamma_0\eta}{k_0}\left(\frac{N_m^{22}}{D_m}\right)\frac{H_m^{(2)}(\gamma_0\rho)}{H_m^{(2)}(\gamma_0\rho_2)} \tag{A3}$$

$$G_{zz}^{(0)} = \frac{j\gamma_0\eta}{k_0}\left(\frac{N_m^{12}}{D_m}\right)\frac{H_m^{(2)}(\gamma_0\rho)}{H_m^{(2)}(\gamma_0\rho_2)} \tag{A4}$$

with

$$D_m = \left(X_m - \epsilon_r\frac{\gamma_0}{\gamma_1}Y_m^{(1)}\right)\left(X_m - \frac{\gamma_0}{\gamma_1}Y_m^{(2)}\right) - \left[(\epsilon_r - 1)\frac{mk_z}{\gamma_0\rho_2}\frac{k_0}{\gamma_1^2}\right]^2 \tag{A5}$$

$$N_m^{11} = (\epsilon_r - 1)\frac{mk_z\rho_2}{(\gamma_1\rho_2)^2} \tag{A6}$$

$$N_m^{12} = X_m - \frac{\gamma_0}{\gamma_1}Y_m^{(2)} \tag{A7}$$

$$N_m^{21} = \frac{\gamma_0}{\gamma_1} Y_m^{(2)} \left[X_m - \epsilon_r \frac{\gamma_0}{\gamma_1} Y_m^{(1)} \right] + (1 - \epsilon_r) \left\{ \frac{mk_z}{\gamma_1^2 \rho_2} \right\}^2 \quad \text{(A8)}$$

$$N_m^{22} = \frac{mk_z}{\gamma_0 \gamma_1 \rho_2} \left[Y_m^{(2)} - \frac{\gamma_0}{\gamma_1} X_m \right] \quad \text{(A9)}$$

and

$$X_m = \frac{H_m^{(2)\prime}(\gamma_0 \rho_2)}{H_m^{(2)}(\gamma_0 \rho_2)} \quad \text{(A10)}$$

$$Y_m^{(1)} = \frac{N_m(\gamma_1\rho_1) J_m'(\gamma_1\rho_2) - J_m(\gamma_1\rho_1) N_m'(\gamma_1\rho_2)}{N_m(\gamma_1\rho_1) J_m(\gamma_1\rho_2) - J_m(\gamma_1\rho_1) N_m(\gamma_1\rho_2)} \quad \text{(A11)}$$

$$Y_m^{(2)} = \frac{N_m'(\gamma_1\rho_1) J_m'(\gamma_1\rho_2) - J_m'(\gamma_1\rho_1) N_m'(\gamma_1\rho_2)}{N_m'(\gamma_1\rho_1) J_m(\gamma_1\rho_2) - J_m'(\gamma_1\rho_1) N_m(\gamma_1\rho_2)}. \quad \text{(A12)}$$

ACKNOWLEDGMENT

The authors wish to thank the reviewers for helpful comments.

REFERENCES

[1] L.-R. Zeng, "A method of solving complicated boundary value problems with its application to coupled rods," *Scientia Sinica*, series A, vol. 25, pp. 1099–1133, Oct. 1982.

[2] L.-R. Zeng and Y. Wang, "Accurate solutions of elliptical and cylindrical striplines and microstrip lines," *IEEE Trans. Microwave Theory Tech.*, vol. MTT-34, pp. 259–265, Feb. 1986.

[3] Y. Wang, "Cylindrical and cylindrically warped strip and microstriplines," *IEEE Trans. Microwave Theory Tech.*, vol. MTT-26, pp. 20–23, Jan. 1978.

[4] K. C. Gupta, R. Garg, and I. J. Bahl, *Microstrip Lines and Slotlines*. Norwood, MA: Artech House, 1979.

[5] N. G. Alexópoulos and S. A. Maas, "Characteristics of microstrip directional couplers on anisotropic substrate," *IEEE Trans. Microwave Theory Tech.*, vol. MTT-30, pp. 1267–1270, Aug. 1982.

[6] A. Nakatani and N. G. Alexópoulos, "Toward a generalized algorithm for the modeling of the dispersive properties of integrated circuit structures on anisotropic substrates," *IEEE Trans. Microwave Theory Tech.*, vol. MTT-33, pp. 1436–1441, Dec. 1985.

[7] N. G. Alexopoulos, P. L. E. Uslenghi, and N. K. Uzunoglu, "Microstrip dipole on cylindrical substrates," *Electromagnetics* vol. 3, nos. 3–4, pp. 311–326, July–Dec. 1983.

[8] A. Nakatani and N. G. Alexópoulos, "Modeling microstrip circuits and microstrip antennas on cylindrical substrates," in *Proc. APS-Symp.*, vol. 1, June 1986, pp. 439–442.

[9] A. Nakatani, N. G. Alexopoulos, N. K. Uzunoglu, and P. L. E. Uslenghi, "Accurate Green's function computation for printed circuit antennas on cylindrical substrates," *Electromagnetics*, vol. 6, no. 3, July-Sept. 1986.

[10] M. Abramowitz and I. A. Stegun, *Handbook of Mathematical Functions*. New York: Dover, 1964.

[11] I. S. Gradshteyn and I. M. Ryzhik, *Table of Integrals, Series, and Products*. New York: Academic Press, 1980.

Nicólaos G. Alexópoulos (S'68–M'69–SM'82–F'87) was born in Athens, Greece, in 1942. He graduated from the 8th Gymnasium of Athens and subsequently obtained the B.S.E.E., M.S.E.E., and Ph.D. degrees from the University of Michigan, Ann Arbor, in 1964, 1967, and 1968, respectively.

He is currently a Professor in the Department of Electrical Engineering, University of California, Los Angeles, Associate Dean of the School of Engineering and Applied Science, and a Consultant with Northrop Corporation's Advanced Systems Division. His current research interests are in electromagnetic theory as it applies to the modeling of integrated-circuit components and printed circuit antennas for microwave and millimeter-wave applications, substrate materials and their effect on integrated-circuit structures and printed antennas, integrated-circuit antenna arrays, and antenna scattering studies. He is the Associate Editor of the *Electromagnetics Journal* and *Alta Frequenza*, and he is on the Editorial Boards of the IEEE TRANSACTIONS ON MICROWAVE THEORY AND TECHNIQUES and the *International Journal on Electromagnetic Theory*.

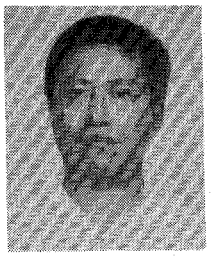

Akifumi Nakatani (S'81) was born in Tokyo, Japan, on February 10, 1956. He received the B.S.E.E. degree from Iwate University, Iwate, Japan, in 1979 and the M.S.E.E. degree from Oregon State University in 1981. He is currently studying at the University of California, Los Angeles, for the Ph.D. degree. His research interests include the computer-aided analysis and design of microwave and millimeter-wave components and printed circuits on curved geometries.